

ON THE NATURE OF THE BOUNDARY RESONANCE ERROR IN NUMERICAL HOMOGENIZATION AND ITS REDUCTION *

SEAN P. CARNEY*, MILICA DUSSINGER†, AND BJÖRN ENGQUIST‡

Abstract. Numerical homogenization of multiscale equations typically requires taking an average of the solution to a microscale problem. Both the boundary conditions and domain size of the microscale problem play an important role in the accuracy of the homogenization procedure. In particular, imposing naive boundary conditions leads to a $\mathcal{O}(\epsilon/\eta)$ error in the computation, where ϵ is the characteristic size of the microscopic fluctuations in the heterogeneous media, and η is the size of the microscopic domain. This so-called boundary, or “cell resonance” error can dominate discretization error and pollute the entire homogenization scheme. There exist several techniques in the literature to reduce the error. Most strategies involve modifying the form of the microscale cell problem. Below we present an alternative procedure based on the observation that the resonance error itself is an oscillatory function of domain size η . After rigorously characterizing the oscillatory behavior for one dimensional and quasi-one dimensional microscale domains, we present a novel strategy to reduce the resonance error. Rather than modifying the form of the cell problem, the original problem is solved for a sequence of domain sizes, and the results are averaged against kernels satisfying certain moment conditions and regularity properties. Numerical examples in one and two dimensions illustrate the utility of the approach.

Key words. multiscale methods, numerical homogenization, boundary resonance error

AMS subject classifications. 35B27, 35B30, 65N06, 74Q05

1. Introduction. This work is concerned with developing methods for the numerical homogenization of the multiscale elliptic equation

$$(1.1) \quad \begin{aligned} -\nabla \cdot (a^\epsilon \nabla u^\epsilon) &= f, & \Omega \subset \mathbb{R}^d \\ u^\epsilon &= g, & \partial\Omega \end{aligned}$$

where $0 < \epsilon \ll 1$, $|\Omega| = \mathcal{O}(1)$, and a^ϵ is assumed to be symmetric, positive-definite, and bounded, so that $\forall w \in \mathbb{R}^d$, $x \neq 0$,

$$(1.2) \quad \lambda |w|^2 \leq \sup_{x \in \Omega} \langle w, a^\epsilon(x) w \rangle \leq \Lambda |w|^2,$$

for some $0 < \lambda < \Lambda < \infty$. a^ϵ is also assumed to oscillate rapidly, that is, with frequencies $\sim 1/\epsilon$, which in turn implies the solution to the elliptic equation u^ϵ is oscillatory as well. Equation (1.1) models, for instance, steady-state heat conduction in a composite material [45], as well as porous media flow through material with highly variable permeability [21].

The mathematical study of the behavior of the solution to (1.1) as $\epsilon \rightarrow 0$ has a long history; see [15, 39, 19]. It is well known that when a^ϵ is periodic, $u^\epsilon \rightarrow \bar{u}$ weakly in $H^1(\Omega)$ and strongly in $L^2(\Omega)$, where \bar{u} satisfies the homogenized equation

$$\begin{aligned} -\nabla \cdot (\bar{a} \nabla \bar{u}) &= f, & \Omega \\ \bar{u} &= g, & \partial\Omega. \end{aligned}$$

*

Funding: This research is supported by National Science Foundation Grant DMS-1620396.

*Department of Mathematical Sciences, George Mason University, Fairfax, VA, 22030, USA; scarney6@gmu.edu

†milicadussinger@gmail.com

‡Department of Mathematics and Oden Institute for Computational Engineering and Sciences, The University of Texas at Austin, Austin, TX, 78712, USA; engquist@oden.utexas.edu

The entries in the homogenized tensor \bar{a} are given by

$$(1.3) \quad \bar{a}_{ij} = \frac{1}{|Y|} \int_Y \left(a_{ij}(y) + a_{ik}(y) \frac{\partial \chi_j}{\partial y_k}(y) \right) dy,$$

where summation over repeated indices is implied, and χ_j solves the cell problem posed in the unit cell $Y = [-1/2, 1/2]^d$

$$(1.4) \quad \begin{aligned} -\nabla \cdot (a \nabla \chi_j) &= \nabla \cdot (a e_j), & Y \\ \chi_j & \text{ } Y\text{-periodic and mean zero,} \end{aligned}$$

and e_j is the standard unit basis vector in \mathbb{R}^d . With a slight modification, a similar result holds for locally periodic media. In $d = 1$, the cell problem reduces to a two-point boundary value problem, and it is easy to show that \bar{a} is given by the harmonic average of a

$$\bar{a} = \left(\int_{-1/2}^{1/2} \frac{1}{a(s)} ds \right)^{-1}.$$

In more general settings, the theory of Γ -convergence provides sufficient conditions for u^ϵ to limit to some \bar{u} ; however, there does not in general exist a closed expression for \bar{a} , and numerical homogenization techniques are required to approximate the homogenized tensor.

There exist many strategies for the numerical homogenization of (1.1); examples include the multiscale finite element method (MsFEM) [37, 36, 24], upscaling techniques [11], the variational multiscale method [1], the heterogeneous multiscale method (HMM) [22, 9], the equation-free method [40], and local orthogonal decomposition (LOD) [42]. Review articles can be found in [33] and [10]. Each method typically involves solving a microscale problem to estimate some missing data from the macroscopic model. Because many examples of realistic heterogeneous media are approximately periodic [18, 28], in practice, both the size of the microscale domain and the boundary conditions prescribed for the microscale problem play an important role in the accuracy of the homogenization procedure.

A common way to study the effect that the choice of microscale domain size and boundary conditions has on numerical homogenization techniques is the setting of periodic oscillations, where analytic results are known, but where the period is assumed to be unknown. In this context, E, Ming, and Zhang [23] first proved that if the microscale problem is solved on a domain whose length η does not coincide with the true period of the heterogeneous media ϵ , a boundary, or ‘‘cell resonance’’ error results that is proportional to ϵ/η and $\epsilon/\eta + \eta$ for truly periodic and locally periodic data, respectively. Yue and E [44] performed a numerical study of this boundary error as a function of domain length η for Dirichlet, Neumann, and periodic boundary conditions and found results consistent with the theory from [23]. Since an $\mathcal{O}(\epsilon/\eta)$ error can potentially dominate discretization error in any sensible numerical homogenization scheme, its reduction can be of great practical importance. One strategy to reduce the cell resonance error is to simply take $\eta \gg \epsilon$. This, however, will of course greatly increase the overall computational cost of the homogenization procedure. Instead, it is preferable to devise strategies to asymptotically reduce the cell resonance error to $\mathcal{O}(\epsilon/\eta)^r$ for some $r > 1$, so that greater accuracy can be obtained at a lower cost.

Several techniques to address the cell resonance error exist in the literature. Most involve the use of smooth, compactly supported averaging kernels, or ‘‘masks’’, when

computing the homogenized coefficients; their compact support helps reduce the influence of the boundary error. The masks are typically inserted into the “data estimation”, or upscaling step of the numerical homogenization procedure, that is, the method-specific analog of (1.3). In the context of the MsFEM, for example, this is called oversampling [35, 38], while in HMM it is called filtering [44, 22]. Although these kernels indeed help reduce the cell resonance error, they only help lower the prefactor in the error’s rate of decay; the rate itself remains proportional to ϵ/η [44, 30]. In [16], however, Blanc and Le Bris proposed to insert the averaging kernels directly in the cell problem (1.4) itself, in contrast to simply utilizing them as post-processing tools. In general this technique helped improve the decay rate of the cell resonance error to second order in ϵ/η .

There are a few other notable examples that modify the form of the cell problem to reduce the influence of the boundary. In [31], Gloria modified the microscale elliptic problem to include a zeroth order term. Since the Green’s function associated to the modified elliptic operator decays exponentially fast, the influence from the boundary is lessened, and a convergence rate of $\mathcal{O}(\epsilon/\eta)^4$ for the cell resonance error was obtained in the periodic setting. The approach was improved in a follow up work [32] using Richardson extrapolation. In [13], Arjmand and Runborg proposed to solve a time-dependent hyperbolic PDE on the microscale, based on the idea that the finite speed of propagation of the initial data prevents the boundary error from affecting the solution in interior of the domain, provided the domain is sufficiently large. Using averaging kernels with special regularity and vanishing moment properties, they were able to rigorously obtain in the periodic setting a convergence rate of $\mathcal{O}(\epsilon/\eta)^q$ for arbitrary q , depending on the regularity properties of the averaging kernel. More recently, Abdulle et al. [2, 3, 4] proposed two separate but related methods to reduce the boundary error. The first approach solves a parabolic microscale problem over a time interval T that depends on the domain length η and the bounds for the oscillatory tensor a (1.2). Similar to [31], the method is based on the exponential decay of the parabolic Green’s function. The second approach solves an elliptic equation with a modified forcing term of the form

$$(1.5) \quad f = \sum_{k=1}^N e^{-\lambda_k T} \langle \nabla \cdot a, \varphi_k \rangle \varphi_k,$$

where $\{\lambda_k, \varphi_k\}_{k=1}^N$ are the first N dominant eigenvalues and eigenfunctions of the operator $A := -\nabla \cdot (a \nabla)$ on $[-\eta/2, \eta/2]^d$ equipped with Dirichlet boundary conditions; this f is a spectral truncation of the solution operator e^{-AT} for the parabolic problem from semigroup theory. With appropriate selections for the parameters T and N , the authors prove exponential decay of the boundary error; see also [5] for an extension to the case of stochastic coefficients.

Rather than modifying the form of the cell problem, we present below an alternative method for reducing the cell resonance error based on the simple observation that, as a function of the microscale domain size η , the error itself is oscillatory. This was observed in the first numerical study of Yue and E; see e.g. Fig. 6 in [44]. One goal of the present work is to more systematically characterize the resonance error as η changes. In dimension $d = 1$ we show that the error can be written

$$(1.6) \quad \frac{1}{x} P(x) + R(x),$$

where $x = \eta/\epsilon$, $P(x)$ is a periodic function, and $R(x)$ is a “corrector” term given by

$$(1.7) \quad R(x) = \sum_{k=2}^{\infty} \left(-\frac{1}{x} P(x) \right)^k.$$

In the case of dimension $d > 1$, a decomposition of the form (1.6) is more difficult to show, as the resonance error depends on the solution to an elliptic problem with boundary data that oscillates as a function of x . The oscillatory boundary condition can lead to complicated boundary layers in the interior; see e.g. [29] and [26]. For two dimensional microscale domains of the form

$$(1.8) \quad I_{\eta} = [-\eta/2, \eta/2] \times [-\epsilon/2, \epsilon/2],$$

we show using Floquet theory [27] that the cell resonance error can also be written in the form (1.6), where the corrector $R(x)$ is given by the average of a locally ϵ -periodic function. More generally for domains of the form $[-\eta/2, \eta/2]^d$ that are relevant to numerical homogenization we offer numerical evidence that something analogous to (1.6) indeed holds, but a fully general theory will likely not be straightforward to develop because of the aforementioned boundary layers.

Based on the oscillatory nature of the cell resonance error, we also describe a technique to asymptotically reduce it by taking a weighted average at several domain sizes. The method is motivated by the form of the one dimensional corrector (1.7), but it is designed to work more generally in higher dimensions. It makes use of averaging kernels that possess regularity properties and vanishing “negative” moment conditions that accelerate the error’s convergence to zero at large domain sizes relative to ϵ . The kernels are similar to, but distinct from, those utilized in [25, 13, 41]. In dimension $d = 1$ we prove the boundary error then decays as

$$(1.9) \quad \mathcal{O}(\epsilon/\eta)^{\min\{p+1, q+3\}}$$

where q and p depend on the regularity and vanishing moment properties of the kernel, respectively. Since the proof only relies on the decomposition (1.7), the result would immediately generalize if (1.7) were shown to hold for $d > 1$. In lieu of a fully general theory, however, we present numerical examples that suggest the strategy indeed is effective in higher dimensions.

As mentioned above, the proposed method does not modify the form of the original cell problem from homogenization theory. Instead, it involves solving a series of microscale problems at different cell sizes η . Hence, there is no need to develop additional approximations to other operators, in contrast to existing methods proposed in the literature. In this regard, the method is well suited to be combined with existing reduced basis (RB) techniques in the numerical homogenization literature [6, 8, 17, 43], where the boundary resonance error is an open problem. Although we do not address this in the current work, we offer some further discussion in [subsection 4.3](#) below.

The remainder of the paper is structured as follows. [Section 2](#) below introduces the space of averaging kernels $\mathbb{K}^{-p, q}$ and some of its properties. Since the results are similar to others available in the literature, their proofs can be found in [Appendix A](#). In [subsection 3.1](#) we derive the expressions (1.6) and (1.7) and then use the averaging kernels to prove the cell resonance error can be asymptotically reduced to (1.9). After deriving an expression for the corrector R in (1.6) for microscale domains of the form (1.8) in [subsection 3.2](#), a numerical strategy for general situations is described in [subsection 3.3](#). Numerical results are presented and discussed in [section 4](#), and then concluding remarks are offered in [section 5](#).

2. Averaging kernels. Let $C(X)$ denote the space of continuous functions on some $X \subseteq \mathbb{R}$, and let $C^k(X)$ be the space of functions that are k times continuously differentiable. For compact X , let $f \in C_0^k(X)$ if f and its k derivatives vanish at the endpoints of X .

DEFINITION 2.1. For $g \in C(\mathbb{R})$ let $g^{[0]}(x) = g(x)$, and define the primitive

$$g^{[k+1]}(x) := \int_0^x g^{[k]}(s) ds + c_{k+1}, \quad k = 0, 1, \dots,$$

where the constant is chosen so that $\int_0^1 g^{[k+1]}(s) ds = 0$.

First, recall the following simple result.

LEMMA 2.2. Let $g \in C(\mathbb{R})$ be 1-periodic, so that $g(x+1) = g(x) \forall x \in \mathbb{R}$, and let g be mean zero, so that $\int_0^1 g(x) dx = 0$. Then the primitive $g^{[1]}(x)$ defined above is also continuous, 1-periodic, and bounded.

The result follows from continuity and the mean-zero assumption; see Appendix A.

Consider next the ‘‘incorrect’’ average of a mean-zero oscillatory function. Let $f \in C(\mathbb{R})$ be 1-periodic, and fix $\epsilon > 0$ and $\eta > \epsilon$ with $\eta/\epsilon \notin \mathbb{N}$. A simple calculation then shows that the error in taking the incorrect average of length η can be bounded as

$$(2.1) \quad \left| \frac{1}{\eta} \int_0^\eta f\left(\frac{x}{\epsilon}\right) dx \right| = \left| \frac{\epsilon}{\eta} \int_0^{\eta/\epsilon - \lfloor \eta/\epsilon \rfloor} f(u) du \right| \leq C \|f\|_\infty \left(\frac{\epsilon}{\eta}\right),$$

where $C = (\eta/\epsilon - \lfloor \eta/\epsilon \rfloor) \in (0, 1)$. Thus, the error decreases like ϵ/η . This error rate can be asymptotically improved, however, if the average is taken against smooth kernels with nice regularity properties.

We next define such averaging kernels that additionally possess vanishing ‘‘negative’’ moments and will be used in the numerical homogenization procedure. These are similar to other kernels with vanishing ‘‘positive’’ moments found the literature; see e.g. [25, 12, 13].

DEFINITION 2.3. Let p and q be nonnegative integers. Define $K \in \mathbb{K}^{-p,q}([1, 2])$ if $K \in C_0^q([1, 2])$, $K^{(q+1)} \in BV([1, 2])$, and

$$(2.2) \quad \int_1^2 K(x) x^{-r} dx = \begin{cases} 1, & r = 0 \\ 0, & r = 1, \dots, p. \end{cases}$$

Note that for $K_\eta(x) := \frac{1}{\eta} K(x/\eta)$, $K \in \mathbb{K}^{-p,q}([1, 2]) \iff K_\eta \in \mathbb{K}^{-p,q}([\eta, 2\eta])$.

The following lemma establishes the bounds needed to prove the main result in subsection 3.1. Since analogous results can be found in the literature for different kernels,* the proof is moved to Appendix A.

LEMMA 2.4. Let $K \in \mathbb{K}^{-p,q}([1, 2])$, and let $K_\eta(x) := \frac{1}{\eta} K(x/\eta)$ for $\eta > 0$. Let $f \in C(\mathbb{R})$ be 1-periodic, and let $\langle f \rangle = \int_0^1 f(s) ds$. Let $0 < \epsilon < \eta$, and for $r \in \mathbb{N}$ let

$$\Upsilon_r(\eta) := \int_\eta^{2\eta} K_\eta(x) x^{-r} f\left(\frac{x}{\epsilon}\right) dx.$$

*See, for example, Lemma 2.3 in [12].

Then:

$$(2.3) \quad |\Upsilon_r(\eta)| \leq \begin{cases} C_1 \|f\|_\infty r^{q+1} \left(\frac{\epsilon}{\eta}\right)^{q+2} \eta^{-r}, & r \leq p \\ C_1 \|f\|_\infty r^{q+1} \left(\frac{\epsilon}{\eta}\right)^{q+2} \eta^{-r} + |\langle f \rangle| \|K\|_\infty \eta^{-r}, & r > p \end{cases}$$

where C_1 is independent of ϵ , η , and r , and depends only on q , K and its derivatives.

For fixed ϵ , Figure 1 compares the decay as a function of η of $\eta^{-r} f(\eta/\epsilon)$ and $\Upsilon_r(\eta)$ for two different periodic functions f ; the rates in Lemma 2.4 are seen to be sharp. The averaging kernels $K \in \mathbb{K}^{-p,q}$ used are of the form

$$(2.4) \quad K(x) = (x-1)^{q+1} (x-2)^{q+1} \sum_{j=0}^p a_j x^j,$$

where the coefficients $\{a_j\}_{j=0}^p$ are chosen to ensure (2.2) holds.

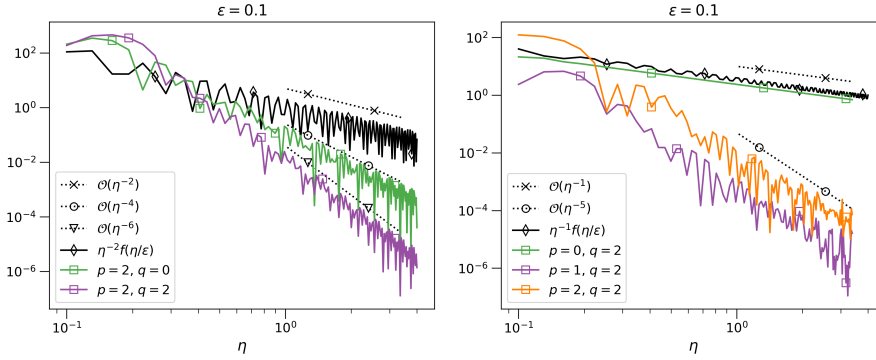


FIG. 1. The decay of $\eta^r f(\eta/\epsilon)$ and $\Upsilon_r(\eta)$ versus η for various averaging kernels $K \in \mathbb{K}^{-p,q}$ of the form (2.4). (Left) $r = 2$ and $f(x) = 1.1 + \sin(2\pi x)$. (Right) $r = 1$ and $f(x)$ is the even periodic extension of the piecewise constant function $\chi_{[0,1/4]} + \chi_{[1/4,1/2]}$.

Having shown the requisite facts for the function class $\mathbb{K}^{-p,q}$, we are now ready to develop our strategy for reducing the boundary error.

3. Reducing the cell resonance error.

3.1. One dimension. Here and throughout the section, let $a : \mathbb{R} \rightarrow \mathbb{R}$ be a 1-periodic, continuous function that satisfies

$$0 < \lambda < a(s) < \Lambda, \quad \forall s \in \mathbb{R}.$$

In one dimension the cell problem (1.4) rescaled by ϵ is

$$(3.1) \quad -\frac{d}{dx} \left(a^\epsilon(x) \frac{d\chi}{dx}(x) \right) = \frac{d}{dx} a^\epsilon(x), \quad x \in [-\epsilon/2, \epsilon/2]$$

χ ϵ -periodic and mean zero

with corresponding homogenized coefficient

$$(3.2) \quad \bar{a} = \left(\frac{1}{\epsilon} \int_{-\epsilon/2}^{\epsilon/2} \frac{1}{a^\epsilon(s)} ds \right)^{-1},$$

where $a^\epsilon(x) = a(x/\epsilon)$. To study the cell resonance error we consider the boundary value problem (3.1) posed instead on the domain $I_\eta = [-\eta/2, \eta/2]$, where η is inconsistent with the periodicity ϵ of the coefficient a^ϵ . The corresponding “incorrect” harmonic average is then

$$(3.3) \quad \left(\frac{1}{\eta} \int_{-\eta/2}^{\eta/2} \frac{1}{a^\epsilon(s)} ds \right)^{-1}.$$

After rescaling the integral by ϵ , the periodic integrand $1/a(s)$ can be decomposed into the sum of odd and even contributions, and since the odd part will vanish by symmetry, (3.3) becomes

$$\left(\frac{2\epsilon}{\eta} \int_0^{\eta/2\epsilon} b_{\text{even}}(s) ds \right)^{-1},$$

where b_{even} denotes the even part of $b(s) := 1/a(s)$. In the development below, we hence assume without loss of generality that b is an even function, and for $\eta > \epsilon/2$ we define the “incorrect” harmonic average

$$(3.4) \quad \rho^\epsilon(\eta) := \left(\frac{\epsilon}{\eta} \int_0^{\eta/\epsilon} b(s) ds \right)^{-1}.$$

After a simple algebraic rearrangement, a calculation similar to (2.1) gives

$$|\bar{a} - \rho^\epsilon(\eta)| \leq C \left(\frac{\epsilon}{\eta} \right),$$

which is the one-dimensional version of the cell-resonance error first derived in [23]. Within this bound, however, the error has a richer structure, which we show next.

LEMMA 3.1. *Let*

$$(3.5) \quad B = \left\| \frac{1}{a} - \int_0^1 \frac{1}{a(s)} ds \right\|_{L^\infty(\mathbb{R})}$$

be the supremum of the fluctuations about the mean for the function $1/a$, and let \bar{a} be the true harmonic average (3.2). If $\eta/\epsilon > \bar{a}B$, then ρ^ϵ is given by the expansion

$$(3.6) \quad \rho^\epsilon(\eta) = \bar{a} \sum_{k=0}^{\infty} \left(-\frac{\epsilon}{\eta} q(\eta/\epsilon) \right)^k$$

where $q(\eta/\epsilon)$ is an ϵ -periodic function of η .

Proof: Let $b(s) := 1/a(s)$, and let $\langle b \rangle := \int_0^1 b(s) ds$ be its arithmetic average. Note $\bar{a} = 1/\langle b \rangle$. Then

$$\begin{aligned} \rho^\epsilon(\eta) &= \left(\langle b \rangle + \frac{\epsilon}{\eta} \int_0^{\eta/\epsilon} (b(s) - \langle b \rangle) ds \right)^{-1} \\ &= \bar{a} \left(1 + \bar{a} \frac{\epsilon}{\eta} \int_0^{\eta/\epsilon} (b(s) - \langle b \rangle) ds \right)^{-1} \\ &= \bar{a} (1 + z(\eta/\epsilon))^{-1}, \end{aligned}$$

where

$$z(\eta/\epsilon) = \bar{a} \frac{\epsilon}{\eta} \int_0^{\eta/\epsilon} (b(s) - \langle b \rangle) ds.$$

The condition $\eta/\epsilon > \bar{a}B$ ensures that $|z(\eta/\epsilon)| < 1$ and hence that ρ^ϵ can be expanded in a uniformly convergent geometric series, as desired. Since $b(s) - \langle b \rangle$ is a mean-zero, periodic function,

$$q(\eta/\epsilon) := z(\eta/\epsilon) \frac{\eta}{\epsilon} = \bar{a} \int_0^{\eta/\epsilon} (b(s) - \langle b \rangle) ds$$

is also ϵ -periodic by Lemma 2.2. \square

The decomposition of the cell resonance error (3.6) motivates the use of weighted averages against kernels $K \in \mathbb{K}^{-p,q}$, which we define next.

DEFINITION 3.2. For $K \in \mathbb{K}^{-p,q}([1, 2])$, $\eta > 0$ and $K_\eta(x) = \frac{1}{\eta} K(x/\eta)$, define

$$(3.7) \quad S^\epsilon(\eta) := \int_\eta^{2\eta} K_\eta(x) \rho^\epsilon(x) dx.$$

The averaged error (3.7) accelerates the convergence of $\rho^\epsilon(\eta)$ to the true harmonic average \bar{a} at a rate that depends on p and q , which we now show.

THEOREM 3.3. For non-negative integers p and q let $K \in \mathbb{K}^{-p,q}([1, 2])$, and let $\epsilon, \eta > 0$ such that

$$(3.8) \quad \bar{a}B \left(1 + \frac{1}{p+1}\right)^{q+1} < \frac{\eta}{\epsilon}$$

where B is given by (3.5) and \bar{a} is the true harmonic average (3.2). Let S^ϵ be defined by (3.7). Then

$$(3.9) \quad |S^\epsilon(\eta) - \bar{a}| \leq C \varphi\left(\bar{a}B \frac{\epsilon}{\eta}\right) \left(\frac{\epsilon}{\eta}\right)^{\min\{p+1, q+3\}},$$

where C depends on p, q, K, \bar{a} and B , and $\varphi(\theta) := 1/(1-\theta)$.

Proof: Since the series expansion (3.6) converges uniformly and absolutely, it can be inserted into the weighted average (3.7), and order of the sum and integral can be interchanged. The resulting expression is

$$\begin{aligned} S^\epsilon(\eta) &= \int_\eta^{2\eta} K_\eta(x) \rho^\epsilon(x) dx \\ &= \bar{a} + \sum_{r=1}^{\infty} (-1)^r \bar{a}^{r+1} \epsilon^r \int_\eta^{2\eta} \left[K_\eta(x) x^{-r} \overbrace{\left(\int_0^{x/\epsilon} (b(s) - \langle b \rangle) ds \right)^r}^{G_r(x/\epsilon)} \right] dx, \end{aligned}$$

which implies

$$(3.10) \quad |S^\epsilon(\eta) - \bar{a}| \leq \sum_{r=1}^{\infty} \bar{a}^{r+1} \epsilon^r \left| \int_\eta^{2\eta} \overbrace{K_\eta(x) x^{-r} G_r(x/\epsilon)}^{F_r} dx \right|.$$

Fixing r , each individual term in the summations can be bounded using [Lemma 2.4](#). Since $b - \langle b \rangle$ is periodic, and mean-zero, and continuous, [Lemma 2.2](#) implies G_r is both periodic and continuous as well. Hence, the assumptions of [Lemma 2.4](#) are indeed satisfied, so that

$$(3.11) \quad F_r \leq \bar{a}^{r+1} \epsilon^r \cdot \begin{cases} C(q, K) \|G_r\|_\infty r^{q+1} \left(\frac{\epsilon}{\eta}\right)^{q+2} \eta^{-r}, & r \leq p \\ C(q, K) \|G_r\|_\infty r^{q+1} \left(\frac{\epsilon}{\eta}\right)^{q+2} \eta^{-r} + |\langle G_r \rangle| \|K\|_\infty \eta^{-r}, & r > p \end{cases}$$

$$= \begin{cases} C(q, K) \|G_r\|_\infty r^{q+1} \bar{a}^{r+1} \left(\frac{\epsilon}{\eta}\right)^{r+q+2}, & r \leq p \\ C(q, K) \|G_r\|_\infty r^{q+1} \bar{a}^{r+1} \left(\frac{\epsilon}{\eta}\right)^{r+q+2} + |\langle G_r \rangle| \|K\|_\infty \bar{a}^{r+1} \left(\frac{\epsilon}{\eta}\right)^r, & r > p. \end{cases}$$

Furthermore, because $b - \langle b \rangle$ is periodic and mean zero,

$$(3.12) \quad \sup_{x \in \mathbb{R}} \left| \int_0^{x/\epsilon} (b(s) - \langle b \rangle) ds \right| \leq B,$$

and hence

$$(3.13) \quad \|G_r\|_\infty \leq B^r;$$

an identical bound exists for $|\langle G_r \rangle|$. The infinite sum [\(3.10\)](#) can be broken up into two pieces, at which point the bounds [\(3.11\)](#) and [\(3.13\)](#) can be inserted to bound the difference between the true harmonic average and $S^\epsilon(\eta)$ by three parts:

$$(3.14) \quad |S^\epsilon(\eta) - \bar{a}| \leq \sum_{r=1}^p C(q, K) r^{q+1} \bar{a}^{r+1} B^r \left(\frac{\epsilon}{\eta}\right)^{r+q+2} + \sum_{r=p+1}^{\infty} \left[C(q, K) r^{q+1} \bar{a}^{r+1} B^r \left(\frac{\epsilon}{\eta}\right)^{r+q+2} + \|K\|_\infty \bar{a}^{r+1} B^r \left(\frac{\epsilon}{\eta}\right)^r \right],$$

The first part on the right hand side (RHS) of the inequality [\(3.14\)](#) is a finite sum, which can be bounded as

$$(3.15) \quad \sum_{r=1}^p C(q, K) r^{q+1} \bar{a}^{r+1} B^r \left(\frac{\epsilon}{\eta}\right)^{r+q+2} \leq C(q, K) \bar{a}^2 B p^{q+2} \left(\frac{\epsilon}{\eta}\right)^{q+3}.$$

The third part of the RHS of [\(3.14\)](#) is the tail of a geometric series. The assumption [\(3.8\)](#) implies

$$(3.16) \quad \sum_{r=p+1}^{\infty} \|K\|_\infty \bar{a} (\bar{a}B)^r \left(\frac{\epsilon}{\eta}\right)^r = \|K\|_\infty \bar{a} (\bar{a}B)^{p+1} \left(\frac{\epsilon}{\eta}\right)^{p+1} \varphi\left(\bar{a}B \frac{\epsilon}{\eta}\right).$$

Finally, the second part of the RHS of [\(3.14\)](#) can be bounded with the ‘‘integral test’’ from elementary calculus, which says

$$\sum_{r=p+1}^{\infty} f(r) \leq f(p+1) + \int_{p+1}^{\infty} f(r) dr,$$

provided f is a monotonically decreasing function of r . Here $f(r) = r^{q+1}(\bar{a}B)^r \left(\frac{\epsilon}{\eta}\right)^r$, and the assumption (3.8) guarantees that $f(r+1) < f(r)$ indeed holds for every $r > p$. Hence

$$(3.17) \quad \sum_{r=p+1}^{\infty} C(q, K) r^{q+1} (\bar{a}B)^r \left(\frac{\epsilon}{\eta}\right)^{r+q+2} \leq C(q, K) \left[(p+1)^{q+1} (\bar{a}B)^{p+1} \left(\frac{\epsilon}{\eta}\right)^{p+q+3} + \left(\frac{\epsilon}{\eta}\right)^{q+2} \underbrace{\int_{p+1}^{\infty} r^{q+1} \alpha^r dr}_{(*)} \right],$$

where $\alpha = \bar{a}B\epsilon/\eta$. The integral (*) can be computed with $q+1$ applications of integration by parts:

$$(3.18) \quad \begin{aligned} (*) &= - \int_{p+1}^{\infty} (q+1)r^q (\log(\alpha))^{-1} \alpha^r dr + (p+1)^{q+1} (-\log(\alpha))^{-1} \alpha^{p+1} \\ &= \int_{p+1}^{\infty} (q+1)! (-\log(\alpha))^{-(q+1)} \alpha^r dr \\ &\quad + \sum_{k=1}^{q+1} \frac{(q+1)!}{(q+2-k)!} (p+1)^{q+2-k} (-\log(\alpha))^{-k} \alpha^{p+1} \\ &= (q+1)! (-\log(\alpha))^{-(q+2)} \alpha^{p+1} \\ &\quad + \alpha^{p+1} \sum_{k=1}^{q+1} \frac{(q+1)!}{(q+2-k)!} (p+1)^{q+2-k} (-\log(\alpha))^{-k} \end{aligned}$$

Comparing the dependence on ϵ/η in the upper bounds on the three parts on the RHS of the inequality (3.14) (given in (3.15), (3.16), and both (3.17) and (3.18)) then gives the desired result:

$$|S^\epsilon(\eta) - \bar{a}| \leq C(p, q, K, \bar{a}, B) \varphi(\bar{a}B \frac{\epsilon}{\eta}) \left(\frac{\epsilon}{\eta}\right)^{\min\{p+1, q+3\}} \quad \square$$

Next we note that in the special case that $K(x) = 1 \in \mathbb{K}^{0,-1}$, (3.7) becomes a simple arithmetic average of ρ^ϵ , and the result (3.9) implies that the averaged error asymptotically decays as ϵ/η . A more direct calculation, however, reveals that this estimate can be improved to second order in ϵ/η .

THEOREM 3.4. *Let $\eta/\epsilon > \bar{a}B$. Then*

$$(3.19) \quad \left| \frac{1}{\eta} \int_{\eta}^{2\eta} (\rho^\epsilon(x) - \bar{a}) dx \right| \leq C \varphi(\bar{a}B \frac{\epsilon}{\eta}) \left(\frac{\epsilon}{\eta}\right)^2$$

where C depends on \bar{a} and B , and $\varphi(\theta) := 1/(1-\theta)$.

Since the proof strategy is similar to that of [Theorem 3.3](#), it is presented in [Appendix B](#).

In practice, we find in the numerical experiments presented in [section 4](#) that $\|K\|_\infty$ grows relatively fast as p and q grow, and hence the error decay rate predicted by (3.9) is not seen until η/ϵ is relatively large. Although the decay rate (3.19) is only second order in ϵ/η , this relatively simple averaging strategy is found to be most effective in practice, particularly in higher dimensions where solving the cell problem (1.4) on a domain with size $\delta := \eta/\epsilon$ in each direction becomes computationally expensive at large δ .

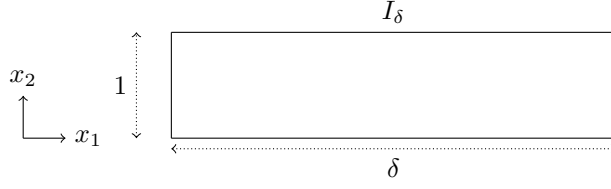


FIG. 2. A two-dimensional “tubular” domain $I_\delta = [-\delta/2, \delta/2] \times [-1/2, 1/2]$, $\delta \notin \mathbb{N}$.

3.2. Tubular domains in two dimensions. Next, let dimension $d = 2$, and in the following assume that $a(x_1, x_2)$ is an isotropic, coercive tensor that is 1-periodic in both arguments. Because we make use of classical Sturm-Liouville theory below, we additionally assume that a is once continuously differentiable.

For $\delta = \eta/\epsilon$, consider domains of the form

$$I_\delta = [-\delta/2, \delta/2] \times [-1/2, 1/2],$$

as depicted in Figure 2. Assume $\delta \notin \mathbb{N}$, so that there is a mismatch between the size of the micro domain and the periodicity of a in the x_1 direction. We show that the cell resonance error can be written in the form (1.6) from the introduction, where the “corrector” $R(\delta)$ is given by the average of a locally ϵ -periodic function.

Consider first the periodic extension to all of \mathbb{R}^2 of the solution χ_j , $j \in \{1, 2\}$, to the true cell problem (1.4) (i.e. with $\delta = 1$). Next consider the solution $\phi_{\delta,j}$ to the cell problem posed on the “incorrect” domain I_δ :

$$(3.20) \quad \begin{aligned} -\nabla \cdot (a \nabla \phi_{\delta,j}) &= \nabla \cdot (a e_j), & I_\delta \\ \int_{I_\delta} \phi_{\delta,j} dx &= 0 \end{aligned}$$

with periodic boundary conditions, and define the difference

$$(3.21) \quad u_{\delta,j}(x_1, x_2) := \phi_{\delta,j}(x_1, x_2) - \chi_j(x_1, x_2).$$

Note that if $\delta \in \mathbb{N}$, then $u_{\delta,j} = 0$ identically. The standard elliptic theory guarantees that both χ_j and $\phi_{\delta,j}$, (and hence $u_{\delta,j}$) are twice continuously differentiable. More generally $u_{\delta,j}$ solves the following elliptic problem in I_δ :

$$(3.22) \quad \begin{aligned} -\nabla \cdot (a \nabla u_{\delta,j}) &= 0, & I_\delta \\ u_{\delta,j}(x_1, -1/2) &= u_{\delta,j}(x_1, 1/2), & x_1 \in [-\delta/2, \delta/2] \\ u_{\delta,j} &= g_{\delta,j}(x_2), & x_1 = -\delta/2 \\ u_{\delta,j} &= h_{\delta,j}(x_2), & x_1 = \delta/2 \end{aligned}$$

where $g_{\delta,j}$ and $h_{\delta,j}$ are simply the difference between $\phi_{\delta,j}$ and χ_j at the points $x_1 = \mp \delta/2$. Since δ is assumed to be inconsistent with the periodicity of a , both g_j and h_j are oscillatory functions of δ for fixed x_2 . Both $u_{\delta,j}$ and $\phi_{\delta,j}$ are of course 1-periodic in x_2 ; we next show that they are also both locally 1-periodic in x_1 .

THEOREM 3.5. *The solution $\phi_{\delta,j}(x_1, x_2)$ to the elliptic problem (3.20) is locally 1-periodic in x_1 .*

Proof: Because χ_j is 1-periodic, it is sufficient to show that the difference $u_{\delta,j} = \phi_{\delta,j} - \chi$ is locally 1-periodic. Since the proof proceeds identically for $j \in \{1, 2\}$, we drop the subscript below for notational convenience.

By assumption of isotropy, the governing equation for u_δ simplifies to

$$(3.23) \quad - \left(\frac{\partial}{\partial x_1} \left(a(x_1, x_2) \frac{\partial}{\partial x_1} \right) + \frac{\partial}{\partial x_2} \left(a(x_1, x_2) \frac{\partial}{\partial x_2} \right) \right) u_\delta(x_1, x_2) = 0.$$

For fixed $x_1 \in \mathbb{R}$, define the symmetric, positive-definite differential operator $L(x_1)$ by:

$$L(x_1)f := - \frac{\partial}{\partial x_2} \left(a(x_1, x_2) \frac{\partial}{\partial x_2} f \right),$$

acting on C^2 functions $f : [-1/2, 1/2] \rightarrow \mathbb{R}$ with periodic boundary conditions. Sturm-Liouville theory [20] guarantees that $L(x_1)$ has a countably infinite set of eigenvalues $\{\lambda_i(x_1)\}_{i=0}^\infty$ that satisfy $\lambda_0(x_1) = 0$ and $\lambda_{i+1}(x_1) > \lambda_i(x_1)$ for all $i \geq 0$, as well as an associated set of complete, mutually orthonormal eigenfunctions $\{\varphi_i(x_1, x_2)\}_{i=0}^\infty$. Note also that by periodicity of a , $L(x_1 + 1) = L(x_1)$ for any $x_1 \in \mathbb{R}$. Since the eigenvalues and their orthonormal eigenfunctions are unique, this implies that both are 1-periodic in x_1 .

Consider an eigenfunction expansion of the solution to the boundary value problem (BVP) (3.22)

$$(3.24) \quad u_\delta(x_1, x_2) = \sum_{i=0}^{\infty} \alpha_i(x_1) \varphi_i(x_1, x_2)$$

where

$$\alpha_i(x_1) = \int_{-1/2}^{1/2} u_\delta(x_1, x_2) \varphi_i(x_1, x_2) dx_2.$$

Since u_δ is C^2 , the expansion converges uniformly and absolutely.

Inserting (3.24) into (3.23) then gives

$$\sum_{i=0}^{\infty} \left[- \frac{\partial}{\partial x_1} \left(a(x_1, x_2) \frac{\partial}{\partial x_1} (\alpha_i(x_1) \varphi_i(x_1, x_2)) \right) + \lambda_i(x_1) \alpha_i(x_1) \varphi_i(x_1, x_2) \right] = 0$$

Let $\psi_i(x_1, x_2) := \alpha_i(x_1) \varphi_i(x_1, x_2)$. A sufficient condition for u to solve (3.23) is for each ψ_i to satisfy the following boundary value problem (BVP) in x_1 that is parameterized by $x_2 \in [-1/2, 1/2]$:

$$(3.25) \quad \begin{aligned} - \frac{\partial}{\partial x_1} \left(a(x_1, x_2) \frac{\partial}{\partial x_1} (\psi_i(x_1, x_2)) \right) + \lambda_i(x_1) \psi_i(x_1, x_2) &= 0, & x_1 \in [-\delta/2, \delta/2] \\ \psi_i &= \beta_i(-\delta/2) \varphi_i(-\delta/2, x_2), & x_1 = -\delta/2 \\ \psi_i &= \gamma_i(\delta/2) \varphi_i(\delta/2, x_2), & x_1 = \delta/2. \end{aligned}$$

Here $\beta_i(-\delta/2)$ is the i -th coefficient in the expansion in eigenfunctions of $L(-\delta/2)$ of the boundary condition $g_\delta(x_2)$ in (3.22), while $\gamma_i(\delta/2)$ is the coefficient of the expansion of $h_\delta(x_2)$ in eigenfunctions of $L(\delta/2)$. Since $\lambda_i(x_1) \geq 0$ for all $i \geq 0$ and $\forall x_1 \in \mathbb{R}$, (3.25) has a unique solution $\forall x_2 \in [-1/2, 1/2]$ and $i \geq 0$.

For each solution $\psi_i(x_1, x_2)$, define the ‘‘flux’’

$$v_i(x_1, x_2) := a(x_1, x_2) \frac{\partial}{\partial x_1} \psi_i(x_1, x_2)$$

and consider a reformulation of the BVP (3.25) into a linear initial value problem system

$$\frac{\partial}{\partial x_1} \begin{pmatrix} v_i(x_1, x_2) \\ \psi_i(x_1, x_2) \end{pmatrix} = \begin{pmatrix} 0 & \lambda_i(x_1, x_2) \\ 1/a(x_1, x_2) & 0 \end{pmatrix} \begin{pmatrix} v_i(x_1, x_2) \\ \psi_i(x_1, x_2) \end{pmatrix}$$

for $x_1 > -\delta/2$, where the initial conditions are simply the values of ψ_i and v_i at $x_1 = -\delta/2$. Since both $1/a$ and λ_i are 1-periodic functions of x_1 , Floquet's theorem [27] implies that the solution can be written as

$$\begin{pmatrix} v_i(x_1, x_2) \\ \psi_i(x_1, x_2) \end{pmatrix} = P_i(x_1, x_2) e^{x_1 K_i(x_2)} c_i$$

for some $c_i \in \mathbb{R}^2$. Here K_i and P_i are both 2×2 matrices that generally depend on x_2 ; however, K_i is constant in x_1 and P_i is 1-periodic in x_1 . Hence, each ψ_i is locally 1-periodic in x_1 . Since the eigenfunction expansion (3.24) converges uniformly and absolutely, the infinite sum $u_\delta = \sum_{i=0}^{\infty} \psi_i$ is also locally 1-periodic in x_1 , as desired. \square

Remark 3.6. Note that while [Theorem 3.5](#) characterizes the behavior of $u_{\delta,j}(x_1, x_2)$ (and hence $\phi_{\delta,j}(x_1, x_2)$) as a function of x_1 for fixed δ , it does not describe the functional dependence on δ . In general the dependence is felt through the oscillatory boundary conditions $g_{\delta,j}$ and $h_{\delta,j}$ in (3.22).

Next, define

$$\rho(\delta) := \frac{1}{\delta} \int_{-\delta/2}^{\delta/2} \int_{-1/2}^{1/2} (a + a \nabla \phi_{\delta,j}) dx_2 dx_1$$

to be the approximation to the homogenized tensor with cell size δ ; the true homogenized coefficients \bar{a} result when $\delta = 1$, or more generally when $\delta \in \mathbb{N}$. As a corollary to [Theorem 3.5](#), we next show the cell resonance error can be written in the form (1.6) from the introduction.

COROLLARY 3.7. *Let $E(\delta) = \rho(\delta) - \bar{a}$ be the cell resonance error. Then*

$$E(\delta) = \frac{1}{\delta} P(\delta) + \frac{1}{\delta} \int_{-\delta/2}^{\delta/2} \zeta(x_1; \delta) dx_1$$

where P is an isotropic tensor that is 1-periodic in δ and ζ is a diagonal tensor that is locally 1-periodic in x_1 .

Proof: First note that since a is isotropic, both \bar{a} and $\rho(\delta)$ are diagonal: $\bar{a}_{ij} = \rho_{ij}(\delta) = 0$ for $i \neq j$. Next, define for $\nu \in \{1, 2\}$ the arithmetic averages

$$\langle a_{\nu\nu} \rangle = \int_{-1/2}^{1/2} \int_{-1/2}^{1/2} a_{\nu\nu} dx_2 dx_1$$

and

$$\left\langle a_{\nu\nu} \frac{\partial \chi_\nu}{\partial x_\nu} \right\rangle = \int_{-1/2}^{1/2} \int_{-1/2}^{1/2} a_{\nu\nu} \frac{\partial \chi_\nu}{\partial x_\nu} dx_2 dx_1$$

(here Einstein summation is not implied), so that $\bar{a}_{\nu\nu} = \langle a_{\nu\nu} \rangle + \langle a_{\nu\nu} \partial \chi_\nu / \partial x_\nu \rangle$. Using $\phi_{\delta,\nu} = u_{\delta,\nu} + \chi_\nu$ from (3.21), the resonance error is given by

$$(3.26) \quad E_{\nu\nu}(\delta) = \frac{1}{\delta} \int_{-\delta/2}^{\delta/2} \int_{-1/2}^{1/2} \left(p_\nu(x_1, x_2) + a_{\nu\nu} \frac{\partial u_{\delta,\nu}}{\partial x_\nu}(x_1, x_2) \right) dx_2 dx_1$$

where

$$p_\nu(x_1, x_2) := (a_{\nu\nu} - \langle a_{\nu\nu} \rangle) + \left(a_{\nu\nu} \frac{\partial \chi_\nu}{\partial x_\nu} - \left\langle a_{\nu\nu} \frac{\partial \chi_\nu}{\partial x_\nu} \right\rangle \right)$$

is a mean-zero, 1-periodic function of both x_1 and x_2 . Let

$$\tilde{p}_\nu(x_1) := \int_{-1/2}^{1/2} p_\nu(x_1, x_2) dx_2,$$

and break \tilde{p}_ν into even and odd parts. Then the first part of (3.26) is

$$\frac{1}{\delta} \int_{-\delta/2}^{\delta/2} \int_{-1/2}^{1/2} p_\nu(x_1, x_2) dx_2 dx_1 = \frac{1}{\delta} 2 \int_0^{\delta/2} \tilde{p}_{\nu, \text{even}}(x_1) dx_1 =: \frac{1}{\delta} P(\delta),$$

and Lemma 2.2 guarantees that the primitive $P(\delta)$ is 1-periodic.

The second term in the resonance error (3.26) is

$$R(\delta) := \frac{1}{\delta} \int_{-\delta/2}^{\delta/2} \int_{-1/2}^{1/2} a_{\nu\nu}(x_1, x_2) \frac{\partial u_{\delta, \nu}}{\partial x_\nu}(x_1, x_2) dx_2 dx_1.$$

By Theorem 3.5, u_ν is locally 1-periodic in x_1 for each δ . Since the gradient ∇u_ν is also locally 1-periodic, setting

$$\zeta_{\nu\nu}(x_1; \delta) := \int_{-1/2}^{1/2} a_{\nu\nu}(x_1, x_2) \frac{\partial u_{\delta, \nu}}{\partial x_\nu}(x_1, x_2) dx_2$$

for $\nu \in \{1, 2\}$ gives the desired result. \square

3.3. General numerical strategy. Motivated by the idea that the cell resonance error is an oscillatory function of domain size, we now propose a numerical strategy for reducing the boundary error in general, higher dimensional settings.

Let the dimension $d > 1$, and for $\eta > 0$, let $I_\eta = [-\eta/2, \eta/2]^d$. Let $a^\epsilon : \mathbb{R}^d \rightarrow \mathbb{R}^d$ to be a bounded, coercive function with entries that are supported at frequencies $\sim 1/\epsilon$. In general a^ϵ need not be periodic. For $1 \leq j \leq d$, let $\chi_{\eta, j}$ be the solution to the elliptic problem

$$\begin{aligned} -\nabla \cdot (a^\epsilon(x) \nabla \chi_{\eta, j}(x)) &= \nabla \cdot (a^\epsilon(x) e_j), & x \in I_\eta \\ \int_{I_\eta} \chi_{\eta, j} dx &= 0 \end{aligned} \tag{3.27}$$

posed with periodic boundary conditions. Other boundary conditions such as Dirichlet or Neumann are possible; however, from [44] it is known that periodic conditions introduce the least boundary effects. In general we assume (3.27) possesses a suitably defined weak solution, but since we are ultimately interested in numerical solutions, we do not further consider any issues of regularity.

Define for $1 \leq i, j \leq d$ the estimate for the homogenized tensor

$$\rho_{ij}(\eta) := \frac{1}{|I_\eta|} \int_{I_\eta} \left(a_{ij}(x) + a_{ik} \frac{\partial \chi_{\eta, j}}{\partial x_k}(x) \right) dx, \tag{3.28}$$

where summation over k is implied. Note that if a^ϵ is ϵ -periodic, for example, the true homogenized coefficient \bar{a}_{ij} is simply given by (3.28) for $\eta = \epsilon$, while if a^ϵ is quasi-periodic or stationary ergodic, then \bar{a}_{ij} is given by the limit as $\eta \rightarrow \infty$ of (3.28),

where $\chi_{\eta,j}$ is replaced by a function $\chi_{\infty,j}$ that solves the elliptic problem (3.27) posed on \mathbb{R}^d [31, 39].

To improve the approximation of the true homogenized coefficients, we introduce the averaged coefficients

$$(3.29) \quad S_{ij}(\eta) := \int_{\eta}^{2\eta} K_{\eta}(t) \rho_{ij}(t) dt,$$

where $K_{\eta} \in \mathbb{K}^{-p,q}([\eta, 2\eta])$ for some nonnegative integers p and q . In practice, this integral is approximated by some quadrature rule defined by M weights $\{\omega_m\}_{m=1}^M$ and nodes $T_M := \{t_m\}_{m=1}^M \subset [\eta, 2\eta]$.

With these preliminary definitions, we now summarize how the smoothed approximation (3.29) of the true homogenized coefficients are obtained in practice.

- (1) For each $t_m \in T_M$:
 - (i) Solve the elliptic problem (3.27) with $\eta = t_m$ for each $1 \leq j \leq d$ using e.g. a finite element method, finite difference method, etc.
 - (ii) Using a quadrature method on I_{t_m} and a suitable estimate for the gradient of $\chi_{t_m,j}$, numerically compute and store $\rho_{ij}(t_m)$ for each $1 \leq i, j \leq d$.
- (2) Using the results, estimate the averaged coefficients S_{ij} with

$$(3.30) \quad \sum_{m=1}^M \omega_m K_{\eta}(t_m) \rho_{ij}(t_m).$$

Numerical examples in two dimensions are described below in Section 4.2.

4. Numerical examples.

4.1. Dimension $d = 1$. We now present some one dimensional numerical examples of the proposed averaging method for reducing the cell resonance error. Since the error can be computed either analytically or with quadrature formulas, it is relatively easy to generate at large values of cell sizes η relative to ϵ and hence detect convergence rates.

Figure 3 compares the cell resonance error (given by the difference between (3.4) and the true harmonic average \bar{a}) with the averaged error (3.7) for various kernels $K \in \mathbb{K}^{-p,q}$. We consider three oscillatory functions $a^{\epsilon}(x)$ given by

$$(4.1) \quad \begin{aligned} a_1^{\epsilon}(x) &= (1.1 + \cos(2\pi x/\epsilon))^{-1} \\ a_2^{\epsilon}(x) &= (2.2 + \cos(2\pi x/\epsilon) + \cos(\sqrt{2}2\pi x/\epsilon))^{-1} \\ a_3^{\epsilon}(x) &= (2 + \text{sign}(\cos(2\pi x/\epsilon)))^{-1}. \end{aligned}$$

The first two examples are smooth, while the third is discontinuous. In all cases the true harmonic average, and, more generally, the incorrect average $\rho^{\epsilon}(\eta)$ are easily computed analytically; note that the second example is quasi-periodic, and hence the true harmonic average is given by (3.4) as $\eta \rightarrow \infty$. The composite trapezoidal rule is used to compute the weighted averages (3.7). We use a large number of quadrature points to ensure the asymptotic decay rates are computed accurately; in particular when $\eta = \epsilon$, $N_{\text{trap}} = 4096$ points are used, and the number of points is increased proportionally as η increases. All kernels $K \in \mathbb{K}^{-p,q}$ that are used are of the form (2.4).

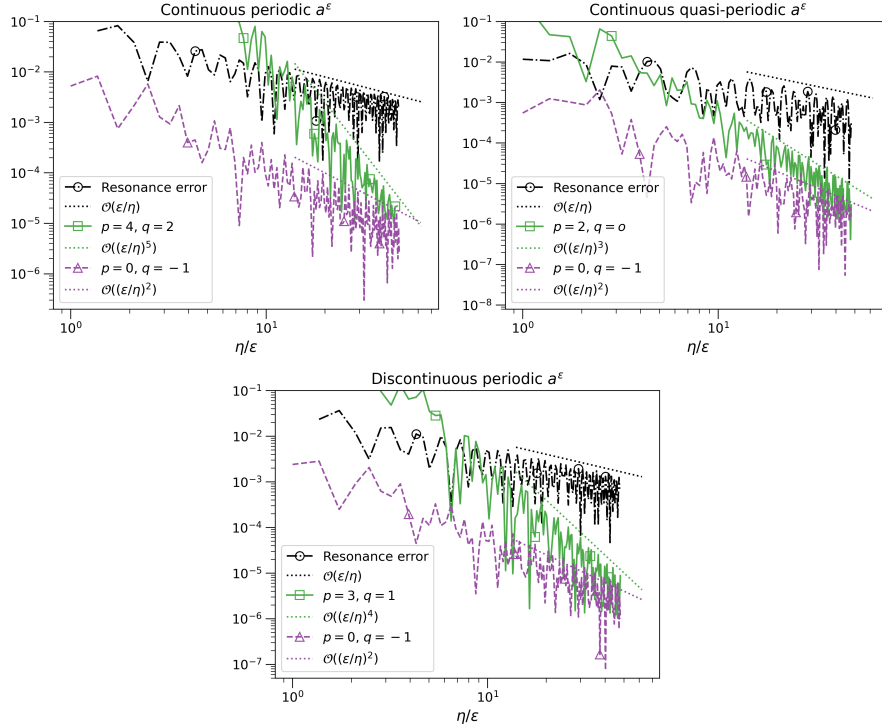


FIG. 3. A comparison of the absolute value of the one-dimensional cell resonance error with the absolute value of the averaged error for various averaging kernels $K \in \mathbb{K}^{-p,q}$ for the three oscillatory functions a^ϵ given in (4.1).

In each case, the cell resonance error of course decays as ϵ/η , while the averaged errors decay at the rates predicted by Theorem 3.3 and Theorem 3.4. Although the convergence rates in ϵ/η are higher for averaging kernels with larger p and q , the constant in front of the asymptotic decay rate also increases. Empirically we find that $\|K\|_\infty$ increases with p and q , which impacts the estimate (2.3) in Lemma 2.4. In contrast, the simple arithmetic average (using $K(x) = 1$) only decreases as $(\epsilon/\eta)^2$ as predicted by Theorem 3.4. However, the asymptotic constant is relatively small, so it still results in a larger decrease of the resonance error even at cell sizes $\eta \sim 50\epsilon$; *a fortiori*, it performs the best at “intermediate” values of η (e.g. $3\epsilon \lesssim \eta \lesssim 10\epsilon$) that are more practical in higher dimensions.

4.2. Dimension $d = 2$. We next present two dimensional numerical computations of the cell resonance error as a function of domain size η that suggest something analogous to the one-dimensional decomposition from Lemma 3.1 indeed holds in higher dimensions.

The cell problems (3.27) on $I_\eta = [-\eta/2, \eta/2]^2$ are solved with a second order finite difference method implemented in C++ with the linear algebra library Eigen [34]. $N = 32$ grid points are used in both the x_1 and x_2 directions for the case $\eta = \epsilon$; as η is increased, N is increased proportionally so that the resolution is approximately constant for each problem. The estimates for the entries in the homogenized tensor $\rho_{ij}(\eta)$ (given by (3.28)) are computed with the composite trapezoidal rule, where the first order partial derivatives in the integrand are approximated with a second order

centered difference formula. The estimates are computed for a sequence of domain sizes between $\eta = \epsilon$ and $\eta = 16\epsilon$ with a spacing of $\Delta\eta = 0.05\epsilon$.

We consider isotropic oscillatory tensors; that is, a^ϵ is given by a (strictly positive) scalar-valued function times the identity matrix. Consider first the ϵ -periodic function

$$(4.2) \quad a^\epsilon(x_1, x_2) = \frac{2 + 1.5 \sin(2\pi x_1/\epsilon)}{2 + 1.5 \sin(2\pi x_2/\epsilon)} + \frac{2 + 1.5 \sin(2\pi x_2/\epsilon)}{2 + 1.5 \sin(2\pi x_1/\epsilon)},$$

taken from Section 3.3 in [44] and visualized in Figure 4 (left). In this case the true homogenized tensor \bar{a} is diagonal but anisotropic. The entries are approximated by solving the cell problem (3.27) for $\eta = \epsilon$ with $N = 1024$ grid points in both the x_1 and x_2 directions, which gives

$$\bar{a} \simeq \begin{pmatrix} 2.34348520086 & 0 \\ 0 & 2.87329450077 \end{pmatrix}.$$

The resonance error $\rho_{ij}(\eta) - \bar{a}_{ij}$ for the two entries $i = j = 1$ and $i = j = 2$ is also shown in Figure 4 (right); between the ϵ/η decay envelopes the error is clearly oscillatory.

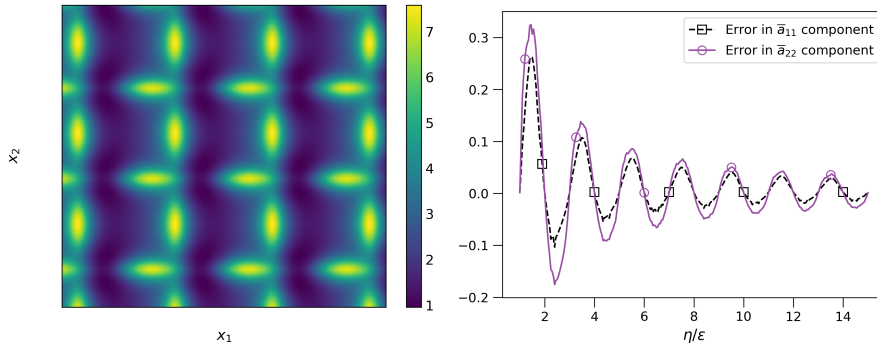


FIG. 4. Visualization of the periodic oscillatory function (4.2) (left) and corresponding components of the cell resonance error as a function of domain size (right).

Figure 5 (right) shows that the resonance error is also oscillatory for the isotropic tensor given by the identity matrix times the quasi-periodic function

$$(4.3) \quad a^\epsilon(x_1, x_2) = (1.1 + \cos(2\pi(x_1 + \sqrt{2}x_2)/\epsilon))^{-1}.$$

As in the the first case, the true homogenized tensor is anisotropic; in this case however the coefficients \bar{a}_{11} and \bar{a}_{22} are approximated by solving (3.27) at relatively large values of η/ϵ . In particular, we take coefficients to be the arithmetic average of the values $\rho_{ij}(\eta)$ from $\eta = 13\epsilon$ to $\eta = 16\epsilon$ which gives

$$\bar{a} \simeq \begin{pmatrix} 1.75643523765 & 0 \\ 0 & 1.34396605902 \end{pmatrix}.$$

Given the oscillatory nature of the cell resonance error as a function of domain size η , we now apply the numerical strategy outlined in subsection 3.3 for its reduction to the cases (4.2) and (4.3). In both cases, the weighted average (3.29) is approximated by the composite trapezoidal rule with intervals of size $\Delta t = 0.05\epsilon$.

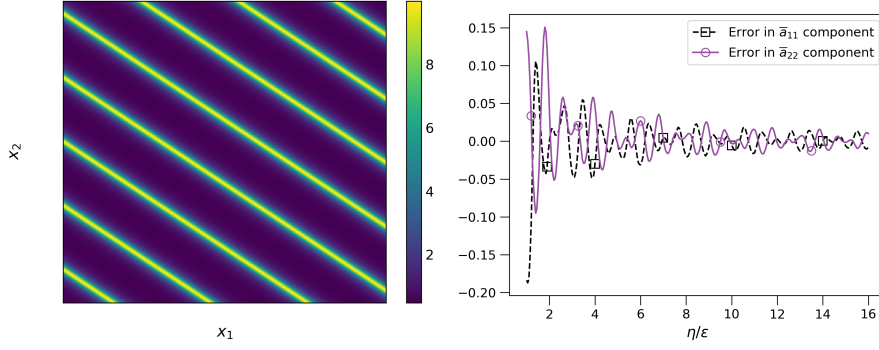


FIG. 5. Visualization of the quasi-periodic oscillatory function (4.3) (left) and corresponding components of the cell resonance error as a function of domain size (right).

Figure 6 shows the results for each of the two components of the resonance error when a^ϵ is given by the ϵ -periodic function (4.2). We consider several types of kernels $K \in \mathbb{K}^{-p,q}$. As discussed in subsection 4.1 for the one dimensional results, kernels with $p \geq 1$ lead to unsatisfactory results at the relatively low values of η/ϵ relevant for dimensions $d \geq 2$ owing to their large ∞ -norms. In contrast, the kernels $K(x) = 1 \in \mathbb{K}^{0,-1}([1, 2])$ and

$$(4.4) \quad K(x) = Ce^{1/((x-1)(x-2))} \in \mathbb{K}^{0,\infty}([1, 2])$$

(where C is chosen so that K has unit mass on $[1, 2]$) reduce the resonance error by an order of magnitude or more at relatively low values of η/ϵ .

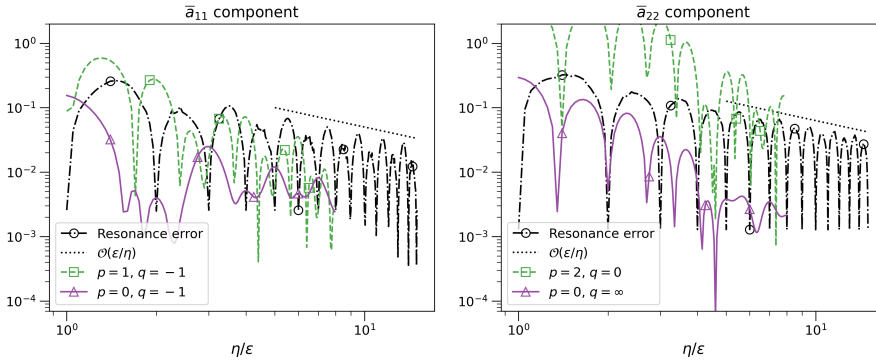


FIG. 6. A comparison of the absolute value of the resonance error with the absolute value of the averaged error for various averaging kernels $K \in \mathbb{K}^{-p,q}$ for the two-dimensional case (4.2).

Figure 7 shows the results for each of the two components of the resonance error when a^ϵ is given by the quasi-periodic function (4.3). In this case we only consider the kernels $K(x) = 1$ and the exponential kernel (4.4). As in the previous example, both reduce the resonance error by several orders of magnitude.

4.3. Computational cost and discussion. Assuming the estimate for the cell resonance error in Theorem 3.3 generalizes to higher dimensions, the computational cost of the method proposed in subsection 3.3 to reduce the error below some tolerance is asymptotically similar to the cost of the hyperbolic microsolver proposed in

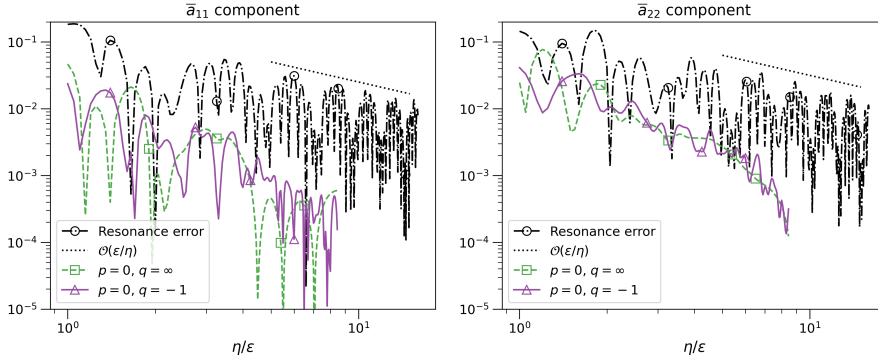


FIG. 7. A comparison of the absolute value of the resonance error with the absolute value of the averaged error for various averaging kernels $K \in \mathbb{K}^{-p,q}$ for the two-dimensional case (4.3).

[13]. Indeed, assume a linear system with N degrees of freedom can be solved with computational cost proportional to N^α ; for example, $\alpha = 2$ (respectively 2.5) for a sparse LU solver in dimension $d = 2$ (resp. $d = 3$). In an ideal scenario, $\alpha = 1$ could be achieved with a multigrid method, however, for microscale domains with diameter η sufficiently large relative to ϵ , it is not clear that the coarse grid solvers can resolve the oscillatory nature of the solution. To generate the approximation (3.29) to the true homogenized coefficients, the method proposed here consists of solving a sequence of elliptic problems on domains with diameters that range from η to 2η . Since (3.28) can oscillate with period ϵ , in general $\mathcal{O}(\eta/\epsilon)$ solves are required. Similarly, for the hyperbolic solver a time step $\Delta t \sim \epsilon$ is required for a total time of integration $T \sim \eta$. Hence, assuming that the total computational cost to estimate the homogenized coefficients (including, e.g. the use of quadrature formulas) is dominated by linear solves, both methods have a total cost proportional to $(\eta/\epsilon)^{\alpha d+1}$. Of course, to be fair it should again be emphasized that the authors in [13] rigorously showed that the resonance error can be made to decay like $(\epsilon/\eta)^s$, where s can be arbitrarily large, while the same can only be said for the current approach in dimension $d = 1$.

Of all the existing techniques in the literature to reduce the cell resonance error, in theory the modified elliptic problem recently proposed in [4] ought to be the most computationally efficient, assuming the Arnoldi iterations used to generate the forcing function f (see Eq. (1.5)) converge sufficiently rapidly; see section 4.3 in [4] for a discussion of this point. As with other analyses found in the literature (see, for example, section 4.1 of [13]), however, this assumes that the cell domain size η is large enough that the theoretical decay rates saturate, which may not be true until $\eta \sim 10\epsilon$ or larger. In practice a microsolver's utility is determined by its performance at relatively low values of η ; depending on the application, this could mean η is several times the assumed local period, or correlation length, ϵ of the heterogeneous media. A comparison of the existing microsolvers in the literature at such “practical” values of η is beyond the scope of the present work, however such a study may be valuable for streamlining research in numerical homogenization, especially if done in collaboration with the engineering community [14].

One advantage of the present approach is that the microscale domain calculations do not communicate with one another, i.e. the microscale solution at a given domain size does not depend on any of the others. The efficiency of the method hence can be greatly increased if the solutions are computed independently in parallel.

Another feature unique to the present approach is that the form of the microscale problem is unmodified from the standard elliptic problem from homogenization theory; there is hence no need to develop approximations for other operators. It is natural then to combine the approach with reduced basis (RB) techniques for numerical homogenization, see for example [7, 8, 17, 43]. Such techniques are important for three dimensional problems, for which the cost of solving microscale problems at every macroscale grid point where homogenized coefficients are needed can be prohibitively expensive. They are also important for optimal control problems constrained by multiscale PDEs. Resolving the boundary resonance error in this context is an open problem, as noted in [6].

Broadly speaking, RB methods precompute in an “offline” stage a low dimensional set of basis functions (say of dimension N) by solving (3.27) at different locations throughout the computational domain Ω . Homogenized coefficients needed by a macrosolver are then efficiently computed in an “online” stage by solving linear systems of size $N \times N$ in the RB space. The strategy described in subsection 3.3 could be used to reduce the resonance error for RB methods by first precomputing M different basis sets, each corresponding to a different domain size t_m , $1 \leq m \leq M$. This of course incurs a larger computational cost in the offline stage, although we again note that this process is parallelizable. Once the different bases are computed, however, the values $\{\rho_{ij}(t_m)\}_{m=1}^M$ in (3.30) can be easily obtained by solving M low dimensional linear systems. We plan to explore this possibility in future research.

5. Conclusions. A novel method for reducing the boundary resonance error in numerical homogenization is proposed. Rather than modifying the form of the microscale problem itself, the method is based on taking a weighted average of the boundary error at a sequence of different microscale domain sizes.

Underlying the method is the observation that the boundary error itself is an oscillatory function of domain size. In one dimensional and two dimensional “tubular” domains the oscillatory nature is rigorously characterized. Numerical evidence suggests the results also hold in more general settings, however, more work is required to rigorously show that this is indeed the case. The problem can be cast as a classical elliptic homogenization problem with oscillatory boundary data, as considered in [29] and [26]; understanding the potentially complicated boundary layers discussed therein is key for further progress in this direction.

Based on the oscillatory nature of the boundary error, we propose solving microscale problems for a sequence of domain sizes and then averaging the results against kernels with vanishing “negative” moments designed to accelerate the convergence of the resonance error to zero at infinitely large microscale domains.

Owing to the rigorous analysis of the behavior of the resonance error, we show for dimension $d = 1$ that the error can be made to decay as $(\epsilon/\eta)^s$ for s arbitrarily large, which we confirm with numerical experiments. However, the method is generally designed for higher dimensions, and numerical examples in $d = 2$ demonstrate its efficacy.

Because the form of the microscale problem is unchanged from classical homogenization theory, the method does not require developing approximations for other operators. In future work, the method could be combined with reduced basis numerical homogenization techniques used for three dimensional problems and for optimization problems with multiscale PDEs as constraints.

Acknowledgments. The authors acknowledge support from the Oden Institute for Computational Engineering and Sciences. We also thank Eric Hester for assistance

with Mathematica calculations to determine the averaging kernels used in some of the numerical examples.

Appendix A. Proof of results for averaging kernels. *Proof of Lemma 2.2:* By continuity of g , both the left and right-handed limits exist for all x :

$$\left| g^{[1]}(x \pm \Delta x) - g^{[1]}(x) \right| \rightarrow 0$$

as $\Delta x \rightarrow 0$, so that $g^{[1]}$ is continuous. Furthermore,

$$\begin{aligned} g^{[1]}(x+1) &= \int_0^{x+1} g(s) ds + c_1 = \int_0^x g(s) ds + c_1 + \int_x^{x+1} g(s) ds \\ &= g^{[1]}(x) + \int_0^1 g(s) ds = g^{[1]}(x) \end{aligned}$$

from the assumption that g is mean zero. Lastly, note that continuous, periodic functions are bounded. \square

The next proof is an adaptation of results from [12].

Proof of Lemma 2.4: Define $F^{[0]}(x) = f(x) - \langle f \rangle$, and let $F^{[q+1]}$ be the $q+1$ primitive, as in Definition 2.1. Note

$$\frac{d^{q+1}}{dx^{q+1}} F^{[q+1]}(x) = F^{[0]}(x),$$

so that

$$(A.1) \quad F^{[0]}(x\eta/\epsilon) = (\epsilon/\eta)^{q+1} \frac{d^{q+1}}{dx^{q+1}} F^{[q+1]}(x\eta/\epsilon).$$

Furthermore, note that $\|F^{[q+1]}\|_\infty \leq 2^{q+1} \|f\|_\infty$. Then after a change of variables,

$$\int_\eta^{2\eta} K_\eta(x) x^{-r} f\left(\frac{x}{\epsilon}\right) dx = \underbrace{\eta^{-r} \int_1^2 K(u) u^{-r} F^{[0]}(u\eta/\epsilon) du}_{(I)} + \underbrace{\langle f \rangle \eta^{-r} \int_1^2 K(u) u^{-r} du}_{(II)},$$

where $F^{[0]}$ is mean-zero. Since $K \in \mathbb{K}^{-p,q}$, (II) vanishes if $r \leq p$; otherwise,

$$\left| \langle f \rangle \eta^{-r} \int_1^2 K(u) u^{-r} du \right| \leq |\langle f \rangle| \|K\|_\infty \eta^{-r}.$$

After using (A.1) and integrating by parts, (I) becomes

$$\begin{aligned} (I) &= (\epsilon/\eta)^{q+1} \eta^{-r} \int_1^2 K(u) u^{-r} \frac{d^{q+1}}{du^{q+1}} F^{[q+1]}(u\eta/\epsilon) du \\ &= (-1)^{q+1} (\epsilon/\eta)^{q+1} \eta^{-r} \int_1^2 \frac{d^{q+1}}{du^{q+1}} (K(u) u^{-r}) F^{[q+1]}(u\eta/\epsilon) du \end{aligned}$$

Since $u^{-r} \in C^\infty([1, 2])$ and by assumption $K^{(q+1)} \in BV([1, 2])$,

$$g(u) := \frac{d^{q+1}}{du^{q+1}} (K(u) u^{-r}) \in BV([1, 2])$$

as well. Changing variables again and breaking the resulting integral in three pieces gives

$$\begin{aligned} (\text{I}) &= (-1)^{q+1} (\epsilon/\eta)^{q+2} \eta^{-r} \int_{\eta/\epsilon}^{2\eta/\epsilon} g(t\epsilon/\eta) F^{[q+1]}(t) dt \\ &= (-1)^{q+1} (\epsilon/\eta)^{q+2} \eta^{-r} \left(\int_{\eta/\epsilon}^{\lceil \eta/\epsilon \rceil} g(t\epsilon/\eta) F^{[q+1]}(t) dt + \int_{\lceil \eta/\epsilon \rceil}^{\lfloor 2\eta/\epsilon \rfloor} g(t\epsilon/\eta) F^{[q+1]}(t) dt \right. \\ &\quad \left. + \int_{\lfloor 2\eta/\epsilon \rfloor}^{2\eta/\epsilon} g(t\epsilon/\eta) F^{[q+1]}(t) dt \right) \end{aligned}$$

The first integral in parentheses can be bounded as

$$\left| \int_{\eta/\epsilon}^{\lceil \eta/\epsilon \rceil} g(t\epsilon/\eta) F^{[q+1]}(t) dt \right| \leq \|g\|_\infty \left\| F^{[q+1]} \right\|_\infty \leq 2^{q+1} \|f\|_\infty V_1^2(g)$$

where $V_1^2(g)$ denotes the total variation of g on $[1, 2]$ and depends only on K , its derivatives, and q . A similar bound exists for the third integral. Next, let $N = \lfloor 2\eta/\epsilon \rfloor - \lceil \eta/\epsilon \rceil$. By construction, $F^{[q+1]}$ is a mean-zero, 1-periodic function, so that

$$\int_{\lceil \eta/\epsilon \rceil}^{\lfloor 2\eta/\epsilon \rfloor} F^{[q+1]}(t) dt = 0.$$

The second integral is then bounded by

$$\left| \sum_{j=1}^{N-1} \int_{\lceil \eta/\epsilon \rceil j}^{\lceil \eta/\epsilon \rceil (j+1)} (g(t\epsilon/\eta) - g(\lceil \eta/\epsilon \rceil j \epsilon/\eta)) F^{[q+1]}(t) dt \right| \leq 2^{q+1} \|f\|_\infty V_1^2(g).$$

Putting it all together, we've shown that

$$\left| \int_{\eta}^{2\eta} K_\eta(x) x^{-r} f\left(\frac{x}{\epsilon}\right) dx \right| \leq 3\eta^{-r} \left(\frac{\epsilon}{\eta}\right)^{q+2} 2^{q+1} \|f\|_\infty V_1^2(g) + |\langle f \rangle| \|K\|_\infty \eta^{-r}$$

for $p < r$ and

$$\left| \int_{\eta}^{2\eta} K_\eta(x) x^{-r} f\left(\frac{x}{\epsilon}\right) dx \right| \leq 3\eta^{-r} \left(\frac{\epsilon}{\eta}\right)^{q+2} 2^{q+1} \|f\|_\infty V_1^2(g)$$

for $p \geq r$, as desired. \square

Appendix B. Proof of Theorem 3.4. *Proof:* Following the proof of [Theorem 3.3](#), we use the expansion (3.6) from [Lemma 3.1](#) and then take the arithmetic average on the interval $[\eta, 2\eta]$. Since the expansion converges absolutely for $\eta/\epsilon > \bar{a}B$, this means

$$(B.1) \quad \frac{1}{\eta} \int_{\eta}^{2\eta} \rho^\epsilon(x) dx - \bar{a} = \bar{a} \sum_{k=1}^{\infty} \frac{1}{\eta} \int_{\eta}^{2\eta} \left(-\frac{\epsilon}{x} q(x/\epsilon)\right)^k dx$$

where

$$q(x/\epsilon) = \bar{a} \int_0^{x/\epsilon} (b(s) - \langle b \rangle) ds.$$

Considering first the $k = 1$ term in the sum and integrating by parts gives

$$\begin{aligned}
 -\frac{1}{\eta} \int_{\eta}^{2\eta} \frac{\epsilon}{x} q(x/\epsilon) dx &= -\frac{1}{\delta} \int_{\delta}^{2\delta} \frac{q(u)}{u} du \\
 \text{(B.2)} \qquad \qquad \qquad &= \frac{1}{\delta} \int_{\delta}^{2\delta} \frac{Q(u)}{u^2} du - \frac{1}{\delta} \left(\frac{1}{2\delta} Q(2\delta) - \frac{1}{\delta} Q(\delta) \right),
 \end{aligned}$$

where $\delta := \eta/\epsilon$ and Q is the primitive of q as defined by [Definition 2.1](#). Since $b(u) - \langle b \rangle$ is a mean-zero periodic function, [Lemma 2.2](#) guarantees that $q(u)$ is also a periodic function. Moreover, since $b(s) = 1/a(s)$ is assumed to be an even function, $q(u)$ is an odd function, and hence

$$\int_{-1/2}^{1/2} q(u) du = 0.$$

Because q is a mean-zero, one-periodic function, [Lemma 2.2](#) implies that Q is also periodic, and hence bounded independently of δ . Ergo, by the triangle inequality [\(B.2\)](#) implies

$$\text{(B.3)} \qquad \left| \frac{1}{\eta} \int_{\eta}^{2\eta} \frac{\epsilon}{x} q(x/\epsilon) dx \right| \leq 2 \|Q\|_{\infty} \left(\frac{\epsilon}{\eta} \right)^2$$

It then remains to consider the $k \geq 2$ terms of the sum in [\(B.1\)](#). As in [\(3.12\)](#) and [\(3.13\)](#),

$$\sup_{x \in \mathbb{R}} |q(x/\epsilon)| \leq \bar{a}B$$

and hence

$$\sup_{x \in \mathbb{R}} |(q(x/\epsilon))^k| \leq \bar{a}^k B^k.$$

We then have

$$\bar{a} \left| \sum_{k=2}^{\infty} \frac{1}{\eta} \int_{\eta}^{2\eta} \left(-\frac{\epsilon}{x} q(x/\epsilon) \right)^k dx \right| \leq \bar{a} \sum_{k=2}^{\infty} (\bar{a}B)^k \left(\frac{\epsilon}{\eta} \right)^k = \bar{a} (\bar{a}B)^2 \left(\frac{\epsilon}{\eta} \right)^2 \varphi(\bar{a}B \frac{\epsilon}{\eta}).$$

Along with [\(B.3\)](#), this gives the desired result.

REFERENCES

- [1] *The variational multiscale method—a paradigm for computational mechanics*, Comput. Methods Appl. Mech. Engrg., 166 (1998), pp. 3 – 24.
- [2] A. ABDULLE, D. ARJMAND, AND E. PAGANONI, *Exponential decay of the resonance error in numerical homogenization via parabolic and elliptic cell problems*, C. R. Math., 357 (2019), pp. 545–551.
- [3] A. ABDULLE, D. ARJMAND, AND E. PAGANONI, *A parabolic local problem with exponential decay of the resonance error for numerical homogenization*, Math. Models Methods Appl. Sci., 31 (2021), pp. 2733–2772.
- [4] A. ABDULLE, D. ARJMAND, AND E. PAGANONI, *An elliptic local problem with exponential decay of the resonance error for numerical homogenization*, Multiscale Model. Simul., 21 (2023), pp. 513–541.
- [5] A. ABDULLE, D. ARJMAND, E. PAGANONI, ET AL., *Mathicse technical report: Analytical and numerical study of a modified cell problem for the numerical homogenization of multiscale random fields*, tech. report, EPFL, 2020.

- [6] A. ABDULLE AND Y. BAI, *Reduced basis finite element heterogeneous multiscale method for high-order discretizations of elliptic homogenization problems*, J. Comput. Phys., 231 (2012), pp. 7014–7036.
- [7] A. ABDULLE AND Y. BAI, *Reduced-order modelling numerical homogenization*, Philos. Trans. Roy. Soc. A, 372 (2014), p. 20130388.
- [8] A. ABDULLE AND P. HENNING, *A reduced basis localized orthogonal decomposition*, J. Comput. Phys., 295 (2015), pp. 379–401.
- [9] A. ABDULLE, E. WEINAN, B. ENGQUIST, AND E. VANDEN-EIJNDEN, *The heterogeneous multiscale method*, Acta Numer., 21 (2012), p. 1–87.
- [10] R. ALTMANN, P. HENNING, AND D. PETERSEIM, *Numerical homogenization beyond scale separation*, Acta Numer., 30 (2021), p. 1–86.
- [11] T. ARBOGAST, *Numerical subgrid upscaling of two-phase flow in porous media*, in Numerical Treatment of Multiphase Flows in Porous Media, Z. Chen, R. E. Ewing, and Z.-C. Shi, eds., Berlin, Heidelberg, 2000, Springer Berlin Heidelberg, pp. 35–49.
- [12] D. ARJMAND AND O. RUNBORG, *Analysis of heterogeneous multiscale methods for long time wave propagation problems*, Multiscale Model. Simul., 12 (2014), pp. 1135–1166.
- [13] D. ARJMAND AND O. RUNBORG, *A time dependent approach for removing the cell boundary error in elliptic homogenization problems*, J. Comput. Phys., 314 (2016), pp. 206 – 227.
- [14] S. BARGMANN, B. KLUSEMANN, J. MARKMANN, J. E. SCHNABEL, K. SCHNEIDER, C. SOYARSLAN, AND J. WILMERS, *Generation of 3d representative volume elements for heterogeneous materials: A review*, Prog. Materials Sci., 96 (2018), pp. 322–384.
- [15] A. BENSOUSSAN, J. LIONS, AND G. PAPANICOLAOU, *Asymptotic Analysis for Periodic Structures*, North-holland, 1978.
- [16] X. BLANC AND C. L. BRIS, *Improving on computation of homogenized coefficients in the periodic and quasi-periodic settings*, Netw. Heterog. Media, 5 (2010), pp. 1–29.
- [17] S. BOYAVAL, *Reduced-basis approach for homogenization beyond the periodic setting*, Multiscale Model. Simul., 7 (2008), pp. 466–494.
- [18] J. CARTWRIGHT, *The impact of 3d seismic data on the understanding of compaction, fluid flow and diagenesis in sedimentary basins*, J. Geolog. Soc., 164 (2007), pp. 881–893.
- [19] D. CIORANESCU AND P. DONATO, *An Introduction to Homogenization*, Oxford University Press, 1999.
- [20] R. COURANT AND D. HILBERT, *Methods of Mathematical Physics*, vol. 1, Wiley, 1937.
- [21] L. J. DURLOFSKY, *Coarse scale models of two phase flow in heterogeneous reservoirs: volume averaged equations and their relationship to existing upscaling techniques*, Comput. Geosci., 2 (1998), pp. 73–92.
- [22] W. E, B. ENGQUIST, X. LI, W. REN, AND E. VANDEN-EIJNDEN, *Heterogeneous multiscale methods: A review*, Commun. Comput. Phys., 2 (2007), pp. 367–450.
- [23] W. E, P. MING, AND P. ZHANG, *Analysis of the heterogeneous multiscale method for elliptic homogenization problems*, J. Amer. Math. Soc., 18 (2005), pp. 121–156.
- [24] Y. EFENDIEV AND T. HOU, *Multiscale Finite Element Methods*, Surveys and Tutorials in the Applied Mathematical Sciences, Springer-Verlag New York, 1 ed., 2009.
- [25] B. ENGQUIST AND Y.-H. TSAI, *Heterogeneous multiscale methods for stiff ordinary differential equations*, Math. Comp., 74 (2005), pp. 1707–1742.
- [26] W. M. FELDMAN, *Homogenization of the oscillating dirichlet boundary condition in general domains*, J. Math. Pures Appl., 101 (2014), pp. 599–622.
- [27] G. FLOQUET, *Sur les équations différentielles linéaires à coefficients périodiques*, in Annales scientifiques de l’École normale supérieure, vol. 12, 1883, pp. 47–88.
- [28] C. W. FREUDIGER, W. MIN, B. G. SAAR, S. LU, G. R. HOLTOM, C. HE, J. C. TSAI, J. X. KANG, AND X. S. XIE, *Label-free biomedical imaging with high sensitivity by stimulated raman scattering microscopy*, Science, 322 (2008), pp. 1857–1861.
- [29] D. GÉRARD-VARET AND N. MASMOUDI, *Homogenization and boundary layers*, Acta Math., 209 (2012), pp. 133–178.
- [30] A. GLORIA, *An analytical framework for numerical homogenization. part ii: Windowing and oversampling*, Multiscale Model. Simul., 7 (2008), pp. 274–293.
- [31] A. GLORIA, *Reduction of the resonance error. Part 1: Approximation of homogenized coefficients*, Math. Models Methods Appl. Sci., 21 (2011), pp. 1601–1630.
- [32] A. GLORIA AND Z. HABIBI, *Reduction in the Resonance Error in Numerical Homogenization II: Correctors and Extrapolation*, Found. Comput. Math., 16 (2016), pp. 217–296.
- [33] GLORIA, ANTOINE, *Numerical homogenization: survey, new results, and perspectives*, ESAIM: Proc., 37 (2012), pp. 50–116.
- [34] G. GUENNEBAUD, B. JACOB, ET AL., *Eigen v3*. <http://eigen.tuxfamily.org>, 2010.
- [35] P. HENNING AND D. PETERSEIM, *Oversampling for the multiscale finite element method*, Mul-

- tiscale Model. Simul., 11 (2013), pp. 1149–1175.
- [36] T. Y. HOU, X. HUI WU, AND Z. CAI, *Convergence of a multiscale finite element method for elliptic problems with rapidly oscillating coefficients*, Math. Comp., (1999), pp. 913–943.
 - [37] T. Y. HOU AND X.-H. WU, *A multiscale finite element method for elliptic problems in composite materials and porous media*, J. Comput. Phys., 134 (1997), pp. 169 – 189.
 - [38] T. Y. HOU, W. XIAO-HUI, AND Y. ZHANG, *Removing the cell resonance error in the multiscale finite element method via a petrov-galerkin formulation*, Commun. Math. Sci., (2004).
 - [39] V. JIKOV, S. KOZLOV, AND O. OLEINIK, *Homogenization of Differential Operators and Integral Functionals*, Springer-Verlag, 1994.
 - [40] I. G. KEVREKIDIS, C. W. GEAR, J. M. HYMAN, P. G. KEVREKIDIS, O. RUNBORG, AND C. THEODOROPOULOS, *Equation-free, coarse-grained multiscale computation: enabling microscopic simulators to perform system-level analysis*, Commun. Math. Sci, 1 (2003), pp. 715–762.
 - [41] L. LEITENMAIER AND O. RUNBORG, *Upscaling errors in heterogeneous multiscale methods for the landau–lifshitz equation*, Multiscale Model. Simul., 20 (2022), pp. 1–35.
 - [42] A. MÅLQVIST AND D. PETERSEIM, *Numerical Homogenization by Localized Orthogonal Decomposition*, SIAM, 2020.
 - [43] N. C. NGUYEN, *A multiscale reduced-basis method for parametrized elliptic partial differential equations with multiple scales*, J. Comput. Phys., 227 (2008), pp. 9807–9822.
 - [44] X. YUE AND W. E, *The local microscale problem in the multiscale modeling of strongly heterogeneous media: Effects of boundary conditions and cell size*, J. Comput. Phys., (2006), pp. 556–572.
 - [45] C. ZWEBEN, *Advances in composite materials for thermal management in electronic packaging*, J. Minerals, Metals & Materials Soc., 50 (1998), pp. 47–51.